# The Study of Assessment Methods for Elastic-Plastic Fracture Process

Y. M. DONG, W. YANG, K. C. HWANG
*Tsinghua University, Beijing, China*

ABSTRACT

A systematic method for assessing the elastic-plastic fracture processes is proposed. The material fracture properties are analytically characterized by two easily measurable fracture parameters. Four different schemes of fracture assessment are presented and checked by the experimental testing data of pressure vessels.

## 1 INTRODUCTION

The current methods for the fracture assessment of pressure vessels have shown the tendency to evolve towards the EPRI methodology (EPRI, 1991, Kumar et al. 1981). Evidences for this unified evolution are indicated by the redrafts of the COD design curve method (see Dalarston, 1986) and the CEGB R6 Failure Assessment Diagram (FAD) method (Milne et al. 1987). The nowaday approach for fracture assessment is also featured by a three stage strategy, namely uses Linear Elastic Fracture Mechanics, Elastic-Plastic Fracture Mechanics for crack initiation and Elastic-Plastic Fracture Mechanics for crack growth instability. For the last, and also the most advanced fracture assessment stage, the following issues have nevertheless not been clarified:

(1) the analytical characterization for the material fracture instability behavior;
(2) simplified analytical forms for elastic-plastic fracture assessment which based on the scientific foundation of ductile fracture mechanics;
(3) a linkage among the major established defect assessment procedures.

It is the aims of the present paper to address the above important issues. We will discuss the theoretical characterization of the fracture resistance curves in the next section, and derive the Two Parameter Method benefited from this essential development. Four different presentations, encompassing all major fracture assessment methodologies, will be described in section 3. The assessment procedure checks well with the testing data of six pre-cracked pressure vessels.

## 2 TWO PARAMETER METHOD

Attention is first focused on the theoretical resistance curve of an elastic power-law plastic (Ramberg-Osgood) material with hardening coefficient A and

hardening exponent n. Based on the Gao-Hwang crack tip singularity solution for such materials under plane strain condition, the following theoretical resistance curve is derived (Luo et al. 1987, Yang 1987, Hwang et al. 1989)

$$\frac{dJ_R^*}{da^*} = (J_R^*/J_{1c}^*)^{1/(n+1)} T_c^* - J_R^{*1/(n+1)}[(\ln J_R^*)^{n/(n-1)} - (\ln J_{1c}^*)^{n/(n-1)}], \tag{1}$$

where the dimensionless quantities with stars are given by

$$J_R^* = \frac{J_{1c}^*}{J_{1c}} J_R , \quad a^* = \frac{b\sigma_o}{\phi m J_{1c} d} (2.718\lambda)^{n/(n+1)} a$$

$$J_{1c}^* = \frac{2.718\lambda}{m\varepsilon_o d} , \quad T_c^* = \frac{2\pi\phi}{b} (2.718\lambda)^{1/(n+1)} T_c . \tag{2}$$

Here, $\sigma_o$, $\varepsilon_o$ and n are material parameters describing a Ramberg-Osgood solid. Parameters b and $\lambda$ (the latter does not denote the plastic flow factor here) depend on the material hardening parameters A and n. These two parameters were tabulated by Luo et al. (1987) for various combinations of A and n through a computation simulation of a remotely J-controlled crack growth. Parameters $\phi$ and d in (2) are connected to the HRR singularity field. A complete parameter tabulation of (1) was also provided by Yang (1987). The factor m relates to the micro-fracture criterion and ranges from 0.5 to 2. Equation (1) and (2) contains only two fracture parameters $J_{1c}$ and $T_c$, namely the J integral and tearing modulus at crack initiation. So the assessment based on this curve is termed "Two Parameter Method". Equation (1) agrees well with the experimental fracture resistance curves of structural steels of relatively low toughness, Hwang et al. 1989.

The applicability of (1) is limited by the following condition which states that the fracture resistance curve should be convex upward :

$$T_c^* < \bar{T}_c^* = \frac{n(n+1)}{n-1} J_{1c}^{*1/(n+1)} (\ln J_{1c}^*)^{1/(n-1)} . \tag{3}$$

Some structural steels with relatively high yield strength, such as 18CrNiWA, satisfies the criterion (3) so that the theoretical prediction of the fracture resistance curve agrees well with the experimental data. On the other hand, structural steels of high toughness, such as A533B-1, fail to obey (3), then substantial deviations occur between the theoretical prediction (1) and the experimental measurement. The reason for the disagreement of high toughness steels lies in that the blunting effect embedded in the first term of (1) from the stationary HRR field should be excluded when formulating a J resistance curve. To achieve that we introduce a reduction factor f in the last expression of (2) to suppress overestimated blunting field represented by $\phi$

$$T_c^* = f\frac{2\pi\phi}{b} (2.718\lambda)^{1/(n+1)} T_c . \tag{4}$$

This factor should be a function of $T_c^*/\bar{T}_c^*$ and bounded from a maximum blunting reduction factor $f_b$ when $T_c^*$ is much greater than $\bar{T}_c^*$, to unity when $T_c^*$ is much less than $\bar{T}_c^*$. A tentative expression for f pertinent to many structural steels is proposed as follows

$$f = \frac{1}{2}[(1 + f_b) + (1 - f_b)\tanh(2.0(\frac{\bar{T}_c^*}{T_c^*} - 1.20))] \tag{5}$$

where the maximum blunting reduction factor represents the ratio of the actual average initial slope of the resistance curve (in a range of crack growth

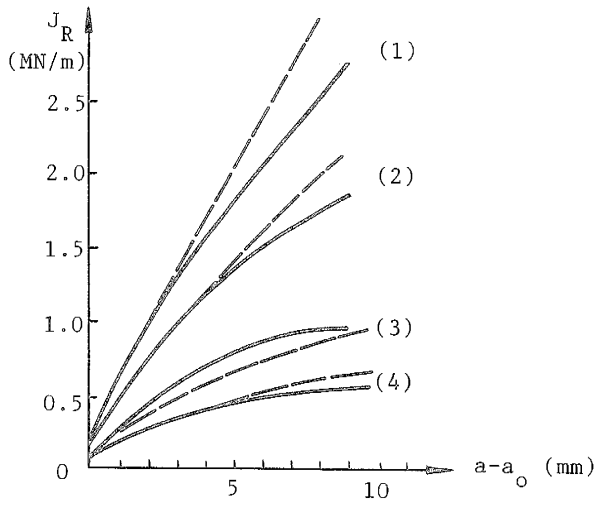


Figure 1 Comparison between theoretical J resistance curves and the expremental measurements of four structural steels. Dashed curves : theoretical predictions; solid curves : experimental measurements. (1) 18MnNiMoNb, (2) A533B-1, (3) 38CrMoAl, (4) 18CrNiWA.

compatable with the blunting increment at initiation) and the slope of the blunting line. After straightforward algebras, we have

$$f_b = 0.4d\varepsilon_o T_c \ . \tag{6}$$

For four typical structural steels, the fracture parameters are listed in Table 1, and the theoretical resistance curves based on them agree well with the experimental measurements, as delineated in Fig.1.

Table 1 Fracture parameters for four structural steels.

| Materials | n | $\sigma_o$ | $J_{1c}$ | $T_c$ | $T_c^*$ | $\bar{T}_c^*/T_c^*$ | $f_b$ | f | $T_c^*$ (modified) |
|---|---|---|---|---|---|---|---|---|---|
| 18MnNiMoNb | 17 | 572 | 0.2 | 267.5 | 52.1 | 0.572 | 0.186 | 0.247 | 12.87 |
| A533B-1 | 10 | 425 | 0.2 | 340 | 78.74 | 0.350 | 0.136 | 0.164 | 12.90 |
| 38CrMoAl | 6.3 | 850 | 0.093 | 53 | 26.5 | 1.18 | 0.035 | 0.493 | 13.10 |
| 18CrNiWA | 22.2 | 1030 | 0.1 | 22 | 3.94 | 8.34 | 0.03 | 1 | 3.94 |

## 3 PRESENTATIONS UNDER DIFFERENT ASSESSMENT SCHEMES

### 3.1 Curve Intersection Approach

We first introduce an assessment methodology parallel to the EPRI common tangent methods of the driving and resistance curves. The essence of this method is to replace the inaccurate tangent construction to a much more accurate curve intersection construction. The basic reference configuration for the fracture assessment is an infinite CCT plate with the half crack length $a_q$. Obviously, the J integral for this reference configuration is a linear function of $a_q$. The dimensionless driving forces $\phi_q$ and $T_q$ are defined by

$$\phi_q = \frac{1}{2\pi}\frac{J_q}{\sigma_o \varepsilon_o a_q} = F_q(\sigma_q) , \qquad T_q = \frac{1}{2\pi\sigma_o\varepsilon_o}\frac{dJ_q}{da_q} \tag{7}$$

and satisfy the condition $\phi_q = T_q$, as suggested by their common linearity to the crack length. For the actual structure components, the dimensionless J integral and tear modulus are

$$\phi = \frac{1}{2\pi}\frac{J}{\sigma_o \varepsilon_o a} = F(\sigma, g) , \qquad T = \frac{1}{2\pi\sigma_o\varepsilon_o}\frac{dJ}{da} \tag{8}$$

where g represents dimensionless geometric parameters. According to the J equivalence principle for crack growth, namely $J = J_q$ when $\sigma = \sigma_q$ (Yang 1987, Dong et al. 1990), the equivalent crack size is given by

$$a/a_q = F_q(\sigma)/F(\sigma, g), \tag{9}$$

and the tearing moduli of the reference and actual configurations are linked by

$$T = T_q \frac{da_q}{da}\Big|_{\sigma} . \tag{10}$$

Combining the driving forces computed here with the resistance curves $\phi_R$ and $T_R$ established in the previous section, one can find the fracture instability point defined by the intersection of $T_R$ and T (as well as $\phi$) curves, as delineated in Fig.2. An example of crack growth instability assessment by curve intersection approach is performed in Fig.3 for SECP specimen. The material selected is A533B-1 with the following parameter settings : A=1.14, n=10, $\sigma_o$ = 425MPa, $\varepsilon_o$=0.2%, $J_{1c}$=0.2MN/m, $T_c$=57.3. The plate has a total width of 0.4m,

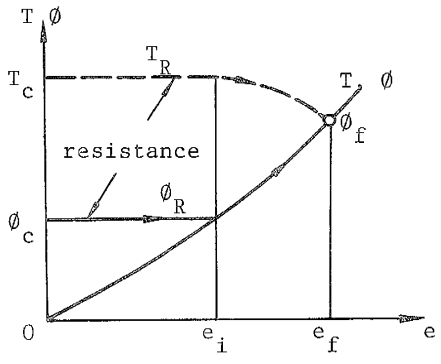


Figure 2 Defect assessment diagram for the basic reference configuration (curve intersection approach).

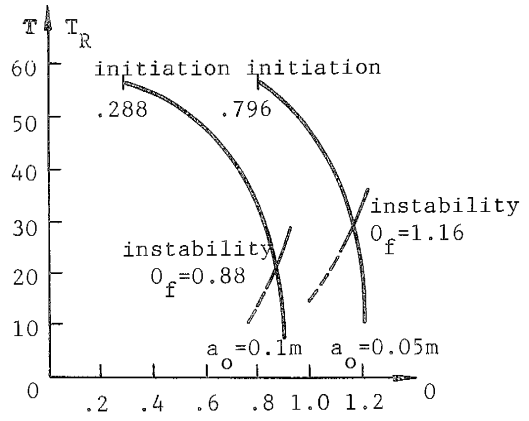


Figure 3 Tearing instability of actual cracked specimen (SECP, plane strain).

and the initial crack lengths are taken as 0.05m and 0.1m respectively. The curve intersection approach is highly accurate (deviation less than 2%).

### 3.2 Design Curve Approach

The previous approach can be further cast into a "design curve" form,

$$\phi(e_f)/y = \frac{C_n}{Y-Ry^{n/(n+1)}} [(\ln(J^*_{1c}y))^{n/(n-1)} - (\ln J^*_{1c})^{n/(n-1)}] \leq \phi_c \qquad (11)$$

where $y = \phi_f/\phi_c$ representing the toughening factor by crack growth, $Y = T_c/\phi_c$ and the revision factor R combines the effect of crack geometry and high strain gradient near the defect region, Yang (1987). Detailed derivation for (11) and the expression of $C_n$ was given by Yang (1987). The shape of the established design curves is described in Fig.4 and compared with the British and Chinese defect assessment codes.

### 3.3 Failure Assessment Diagram

Based on the same development which connects the EPRI approach to the failure assessment diagram, one can cast the present two-parameter assessment scheme in terms of the CEGB/R6 methodology. The details are given by Yang et al. (1988).

### 3.4 Admissible Stress Curve

An admissible stress curve refers to the stress-crack growth curve $\sigma(a)$ admissible by the J resistance. Accordingly, the function

$$D(\sigma,a) = J(a,\sigma(a)) - J_R(a-a_o) \qquad (12)$$

should be identically zero. Differentiating (12) with respect to the crack length a and setting the derivative as zero, one finds (Dong et al. 1990)

$$T|_\sigma = T_R \quad \text{provided} \quad d\sigma(a)/da = 0. \qquad (13)$$

Namely the peak of the admissible stress curve represents the failure stress

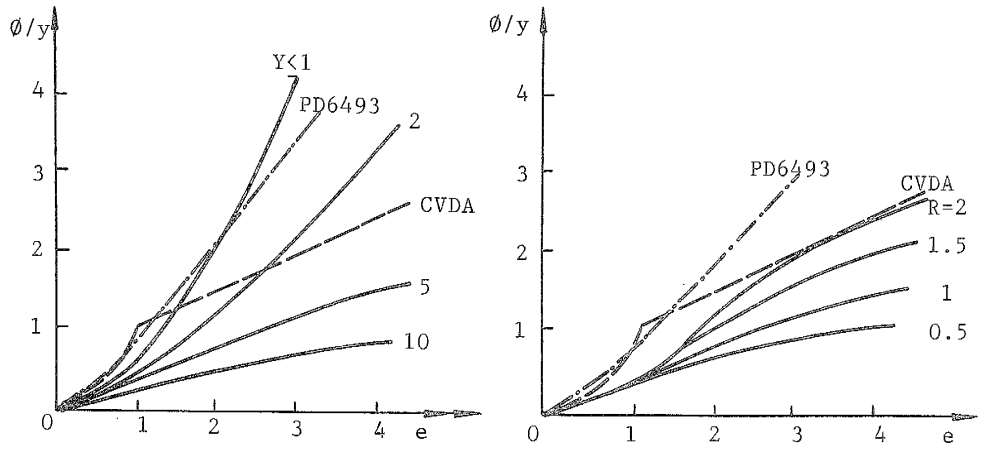


Figure 4 Computed design curves (without safety margin), left R=1, right Y=5.

at tearing instability and the maximum attainable crack growth amount. We examplify this approach by pressure vessels made of low-carbon seamless steel with axial cracks along the vessel exteriors. The material characterization for the vessel material is :

$$\sigma_o = 256\text{MPa}, \quad E = 2.08\text{x}10^5\text{MPa}, \quad A = 1.00, \quad n = 6.582,$$

$$J_R = 1.903 \left(\frac{a-a_o}{1\text{meter}}\right)^{0.414} \text{MN/m} \tag{14}$$

After plotting the stress admissible curves for six different geometries of cracked vessels, we are able to predict the burst pressures of them as shown in the 4th row of Table 2. Those theoretical predictions agree well with the experimental meauments made on those cracked vessels (Zhang and Wang, 1987).

Table 2 Defect assessment by stress admissible method for six precracked pressure vessels

| No. | $R_i/R_o$ | $a_o/b$ | Burst Pressure (predicted) | Burst Pressure (measured) | error% | Stable Crack Growth mm |
|---|---|---|---|---|---|---|
| 1 | 59.5/68.65 | 0.595 | 25.6 MPa | 23.6 MPa | 8.8 | 0.30 |
| 2 | 59.5/68.4 | 0.663 | 22.0 MPa | 20.1 MPa | 9.4 | 0.30 |
| 3 | 59.5/68.65 | 0.524 | 28.9 MPa | 31.0 MPa | -6.8 | 0.35 |
| 4 | 59.5/71.4 | 0.597 | 33.5 MPa | 34.8 MPa | -3.7 | 0.40 |
| 5 | 59.5/71.4 | 0.609 | 32.8 MPa | 33.7 MPa | -2.7 | 0.40 |
| 6 | 59.5/71.4 | 0.489 | 39.9 MPa | 37.9 MPa | 5.3 | 0.50 |

Acknowledgement The authors thank for the supports from the National Natural Science Foundation of China and from National Nuclear Safety Administration.

## REFERENCES

Darlaston,B.J. (1986). Pressure Vessel Technology and Associated Topics, ECICT2/4A.

Dong,Y.M., Yang,W. and Hwang,K.C. (1990). Fat. & Fract. Eng. Mat. & Struct., Vol.13, pp.399-410.

EPRI (1991). Ductile Fracture Handbook, Vol.1,2,3.

Hwang,K.C. et al. (1989). Proc. SMiRT 10, Vol.G, pp.77-80.

Kumar,V., German,M.D. and Shih,C.F. (1981). An Engineering Approach for Elastic Plastic Fracture Analysis, EPRI Report NP-1931, EPRI.

Luo,X., Yang,W. and Hwang,K.C. (1987). Proc. ICFFM, pp.277-281.

Milne,I., Ainsworth,R.A. and Stewart,A.T. (1986). Assessment of the Integrity of Structures Containing Defects, CEGB Report R/H/R6-Revision 3.

Yang,W. (1987). Acta Mechanica Sinica, Vol.3, pp.342-352.

Yang,W. et al. (1988). Proc. of ICPVT6, pp.819-826.

Zhang,K.D. and Wang,W. (1987). Int. J. Press. Vess. Piping, Vol.27, pp.223-234.